Title: A late Holocene multiproxy fire record from a tropical savanna, eastern Arnhem Land, Northern Territory, Australia

Authors:

Emma Rehn [1,2,*], Cassandra Rowe [1,2], Sean Ulm [2,3], Craig Woodward [4] and Michael Bird [1,2]

[1] College of Science and Engineering, James Cook University, PO Box 6811, Cairns QLD 4870, Australia.
[2] ARC Centre of Excellence for Australian Biodiversity and Heritage, James Cook University, PO Box 6811, Cairns QLD 4870, Australia.
[3] College of Arts, Society and Education, James Cook University, PO Box 6811, Cairns QLD 4870, Australia.
[4] NSTLI The Environment, Australian National Science and Technology Organisation, New Illawarra Road, Lucas Heights NSW 2234, Australia.
* Correspondence: emma.rehn@my.jcu.edu.au

0. Abstract

Fire has a long history in Australia and is a key driver of vegetation dynamics in the tropical savanna ecosystems that cover one quarter of the country. Fire reconstructions are required to understand ecosystem dynamics over the long term but these data are lacking for the extensive savannas of northern Australia. This paper presents a multiproxy palaeofire record for Marura sinkhole in eastern Arnhem Land, Northern Territory, Australia. The record is constructed by combining optical methods (counts and morphology of macroscopic and microscopic charcoal particles) and chemical methods (quantification of abundance and stable isotope composition of pyrogenic carbon by hydrogen pyrolysis). This novel combination of measurements enables the generation of a record of relative fire intensity to investigate the interplay between natural and anthropogenic influences. The Marura palaeofire record comprises three main phases: 4600-2800 cal BP, 2800-900 cal BP and 900 cal BP to present. Highest fire incidence occurs at ~4600-4000 cal BP, coinciding with regional records of high effective precipitation, and all fire proxies decline from that time to the present. 2800-900 cal BP is characterised by variable fire intensities and aligns with archaeological evidence of occupation at nearby Blue Mud Bay. All fire proxies decline significantly after 900 cal BP. The combination of charcoal and

pyrogenic carbon measures is a promising proxy for relative fire intensity in sedimentary records and a useful tool for investigating potential anthropogenic fire regimes.

Keywords: tropical savannas; charcoal; pyrogenic carbon; relative fire intensity; late Holocene; northern Australia

1. Introduction

Fire has a long history in shaping Australian ecosystems (e.g. Hiscock and Kershaw 1992; Johnson 2016; Kershaw et al. 2002). While humans became an ignition source for fires in Australia at least 60,000 years ago (Clarkson et al. 2017), the role of humans in shaping fire regimes over millennial timescales is debated (e.g. Black, Mooney and Haberle 2007; Enright and Thomas 2008; Mooney et al. 2011; Williams et al. 2015). Some Australian landscapes encountered by Europeans in the eighteenth century were carefully managed, although the extent and timescale of this management is poorly known (Pyne 1991; Gammage 2012). Studies such as Mooney et al. (2011) and Williams et al. (2015) suggest that at a continental scale, climate was a more important driver of biomass burning than humans in Australia, with the exception of the last 200 years. These conclusions do not preclude anthropogenic drivers on local or smaller regional scales, or effects on fire regime variables other than total biomass burnt. Understanding this combination of driving forces is critical to investigating the tropical savanna landscapes of northern Australia, as fire is "a prime mover of savanna dynamics" (Pyne 1991, p.61). The savannas of northern Australia cover approximately one quarter of the continent (Fox et al. 2001), with up to 50% of these savannas burning each year (Andersen, Cook and Williams 2003, p.vii). Research in Australia's tropical savannas is critical to determine long-term dynamics between fire, climate, humans and vegetation in northern Australia.

The late Holocene (4200 BP to present; International Commission on Stratigraphy 2019) is a period climatically comparable to modern conditions. During the mid-to-late Holocene in northern Australia, the El Niño-Southern Oscillation (ENSO) developed (Diaz and Markgraf 1992), sea-levels stabilised after a high-stand of 0.7 to 1.6 metres in the mid-Holocene (Lewis et al. 2013; Sloss et al. 2018), and the Indonesian-Australian Summer Monsoon weakened (Wyrwoll and Miller 2001). Multiple sites across northern Australia show evidence of vegetation disturbance during the late Holocene, attributed to ENSO-driven changes in climate (e.g. storms and drought) and/or human activity (Haberle 2005; Prebble et al. 2005; Proske and Haberle 2012; Rowe 2007), as Indigenous populations expanded (Williams 2013). In addition, the late Holocene encompasses the transition from palaeoenvironmental to historical timescales, a period that is critical for enabling comparisons between palaeoenvironmental proxy records and current fire regimes to inform modelling and management (e.g. Aleman et al. 2013; Ekblom and Gillson 2010; Higuera, Sprugel and Brubaker 2005; Perry, Wilmshurst and McGlone 2014). The historical period begins in northern Australia with the first recorded European contact in the 17th century (Heeres 1899).

Fire proxy data are limited for the tropical savannas of northern Australia compared to the relatively well-studied temperate southeast of Australia (Mooney et al. 2011). Many key regions such as Arnhem Land in the Northern Territory lack published palaeoenvironmental records of any kind. Of the palaeoenvironmental records that do exist for northern Australia, few include fire proxies. Our understanding of the evolution of fire regimes, and the influence of humans and climate, in this area is therefore limited.

Improving our understanding of past fire dynamics in Australia requires not only additional records to fill geographical gaps but also methodological improvements in the creation and interpretation of fire proxy data. The use of sedimentary charcoal counts to reconstruct fire

histories began in the 1940s (see Iversen 1941) and has been widely applied since then (e.g. Mooney et al. 2011). A range of methods have been developed to obtain more nuanced information from charcoal analysis than a single measure of accumulation or influx (for an overview, see Mooney and Tinner 2011). Size differentiation to determine source area (Clark 1988; Peters and Higuera 2007) and analysis of the morphological characteristics of particles to distinguish fuel (vegetation) type are becoming more routine (Aleman et al. 2013; Courtney Mustaphi and Pisaric 2014; Crawford and Belcher 2014; Enache and Cumming 2006; Leys, Commerford and McLauchlan 2017; Umbanhowar and McGrath 1998). Separation of charcoal particles into macroscopic and microscopic size fractions to distinguish local/watershed and extra-local/beyond the watershed signals, respectively, is commonly used in Australian palaeofire studies (e.g. Haberle 2005; Proske and Haberle 2012; Stevenson et al. 2015). However, the size threshold for separating macroscopic and microscopic charcoal is debated (e.g. >50 µm, Duffin, Gillson and Willis 2008; >100 µm, Mooney and Tinner 2011; >125 µm, Stevenson and Haberle 2005; >150 µm, Ekblom and Gillson 2010; >250 µm, Black and Mooney 2006) and the usefulness of this method has been questioned due to potential correlation between macroscopic size fractions (see Mooney and Tinner 2011; Leys et al. 2015). Characterisation of fuel composition using particle aspect ratios or classification into categories based on morphology (morphotypes; e.g. Enache and Cumming 2006) has received minimal attention in Australian studies and its utility in Australian contexts is therefore unknown.

The chemical isolation of pyrogenic carbon (using the hydrogen pyrolysis method) is a relatively recent technique in palaeofire research developed by Ascough et al. (2009), Meredith et al. (2012) and Wurster et al. (2012, 2013). Fire generates a continuum of combustion products from partially charred biomass to refractory soot, with increasing temperatures associated with products of increasing aromaticity and decreasing reactivity (Masiello 2004).

Charcoal is produced under a range of fire conditions, and changes in fire temperature and intensity may generate variations in physical and chemical properties of charcoal (Mooney and Tinner 2011). The hydrogen pyrolysis method isolates refractory carbonaceous material of >7 polyaromatic rings (referred to here as pyrogenic carbon) from labile carbon in a sample (Ascough et al. 2009; Meredith et al. 2012). Pyrogenic carbon content of charcoal increases with increasing temperature (Bird and Ascough 2012). Pyrogenic carbon therefore represents a consistent portion of the continuum of combustion products at the higher temperature (and lower reactivity) end of the spectrum (Meredith et al. 2012) and is potentially a complementary fire proxy to charcoal, representing lower temperatures and higher reactivity (Masiello 2004).

A combined application of hydrogen pyrolysis and charcoal counting methods is presented by Bird et al. (2019), demonstrating positive correlations between microscopic charcoal concentration and pyrogenic carbon abundances (% by weight) for “modern” and “Holocene" representative samples from sites across the Northern Territory. Bird et al. (2019) also demonstrated the effectiveness of the carbon isotope abundance of pyrogenic carbon as a proxy recording the relative tree-grass composition of biomass burnt. This composite optical and chemical palaeofire approach has not been applied to a Quaternary record prior to this study, with the exception of Thevenon et al. (2010). While Bird et al. (2019) found positive correlations between charcoal and pyrogenic carbon abundances, Thevenon et al. (2010) showed variations between these measures but did not address or interpret those variations. As pyrogenic carbon is present in greater abundances in charcoal formed under higher burn temperatures, differences in the relative influx of these combustion products potentially reflect changes in fire intensity (a combination of temperature and residence time; Keeley 2009). This paper presents a method utilising differences in charcoal and pyrogenic carbon influxes to estimate relative fire intensity.

This paper presents a new multiproxy palaeofire record for Marura sinkhole in eastern Arnhem Land (Figure 1). Marura forms part of a series of Quaternary study sites across the "Top End" of the Northern Territory, introduced by Bird et al. (2019), with the first record presented by Rowe et al. (2019) for Girraween Lagoon. This paper presents the first fire proxy record for Arnhem Land - a region larger than Portugal. This study also serves as a test of fire reconstruction techniques to determine their applicability to Australian tropical savannas, including the potential benefits of a multiproxy approach.

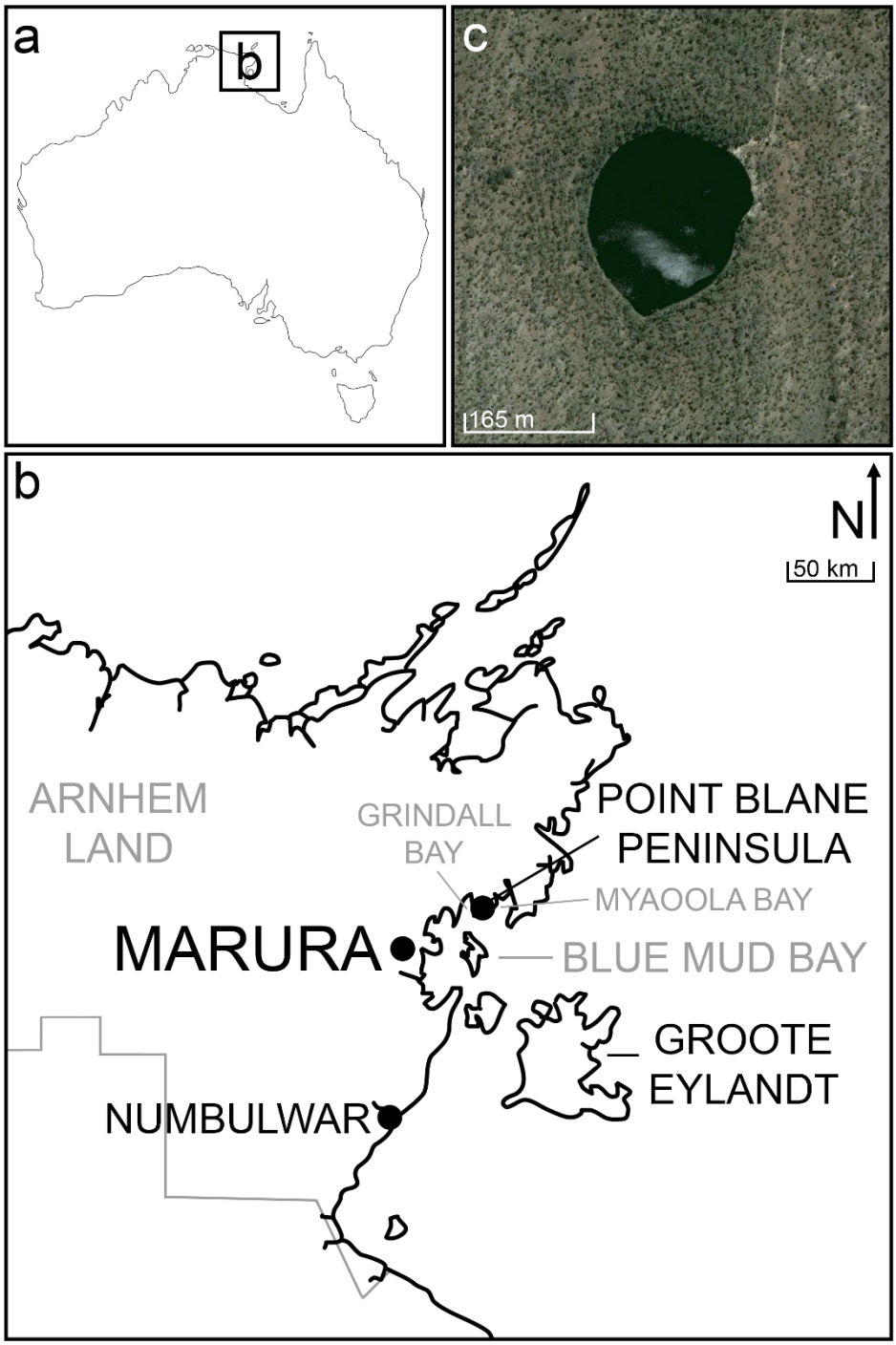

1

2 Figure 1: Map of the study area, showing a) location of the study area in Australia, b) key locations
3 mentioned in the text (including the approximate boundary of Arnhem Land marked in grey), and c)
4 satellite image of Marura sinkhole (after Google Earth 2020).

5

2. Site Description

Marura (13.409°S, 135.774°E) is a freshwater lake in a sinkhole at 50 m a.s.l., located approximately 9.5 km inland from Blue Mud Bay in eastern Arnhem Land, Northern Territory, Australia (Figure 1). The circular feature is approximately 190 m in diameter with a small catchment area of approximately 0.2 km² and a water depth of between 11 and 12 m (measured 2014-2015). The resistivity profile for Marura is presented in Bird et al. (2019, p.238), which shows soft, low resistivity sediment underlain by basement rock with high resistivity. The traditional owners of this land are the Ritharrngu, part of the Yolngu language group (Gambold 2015).

2.1 Climate and Geology

The climate of the region is strongly influenced by the Indonesian-Australian Summer Monsoon (IASM), and interannual shifts of the Intertropical Convergence Zone (ITCZ) driven by the El Niño-Southern Oscillation (ENSO) (see Diaz and Markgraf 1992; Wyrwoll and Miller 2001). Mean annual rainfall is 1290 mm, measured from the nearest weather station at Groote Eylandt Airport approximately 98 km southeast of Marura (Bureau of Meteorology [BOM] 2020). Rainfall is highly seasonal and most (>90 %) occurs between November and April (BOM 2020). Winds are predominantly from the west-northwest and southeast in January and July, respectively (BOM 2020). Average daily temperature ranges from 15.1 °C in the coldest month (August) to 34.5 °C in the warmest month (November) (BOM 2020). As a potential fire ignition source, eastern Arnhem Land has an average annual lightning (cloud-to-ground) flash density of 2-3 flash/km^2/year, primarily coinciding with the wettest months of the year (Dowdy and Kuleshov 2014).

The site is underlain by the Bath Range formation of the Balma Group comprised of dolomitic siltstone, sandstone, dolarenite, and evaporitic-stromatolitic dolostone (Haines et al. 1999), an area of which dissolved to form Marura sinkhole by collapsing into an underlying void. This unit is partly overlain by Cenozoic to Holocene unconsolidated sediments and laterite duricrust (Haines et al. 1999). Marura is located on the eastern edge of the Gulf Fall land unit, a dissected landscape drained by streams into the Gulf of Carpentaria (Plumb and Roberts 1967, p.4). Soils include shallow stony sands associated with slopes and plains of yellow earthy sands and soils (Northcote et al. 1960-1968).

Marura's small catchment area is due to the sinkhole's semi-encircled formation within the landscape. The terrain visibly slopes towards the sinkhole close to the southern edge of the site, with an average elevation of ~43 m a.s.l. on the eastern side up to ~63 m a.s.l. on the southern side.

2.2 Vegetation and Fire

Vegetation immediately surrounding Marura is open eucalypt forest with a grassy understorey, characterised by dominant *Eucalyptus tetrodonta* and *E. miniata*, with species of *Acacia*, *Calytrix* and *Callitris intratropica* in the subcanopy (Figure 2) (Department of the Environment and Energy 2017). Canopy cover varies between 20 and 50% in the upper tree layer (Department of the Environment and Energy 2017). Ground cover is dominated by grasses; these are variable in their distribution, being thinner to patchy to the north where soils are shallow. This same woodland extends downslope to the waterline at Marura, incorporating higher tree density and a more obvious shrub layer with species such as *Livistona humilis*. The sloping terrain on the southern side of the sinkhole, and its direct drop into the sinkhole pool, has meant *Melaleuca* fringes and/or swampy-sedge wetland edges are absent at Marura.

Aquatics, including submerged floating plants, were not observed at the time of fieldwork, likely due to rapidly increasing water depth away from the lake shore.

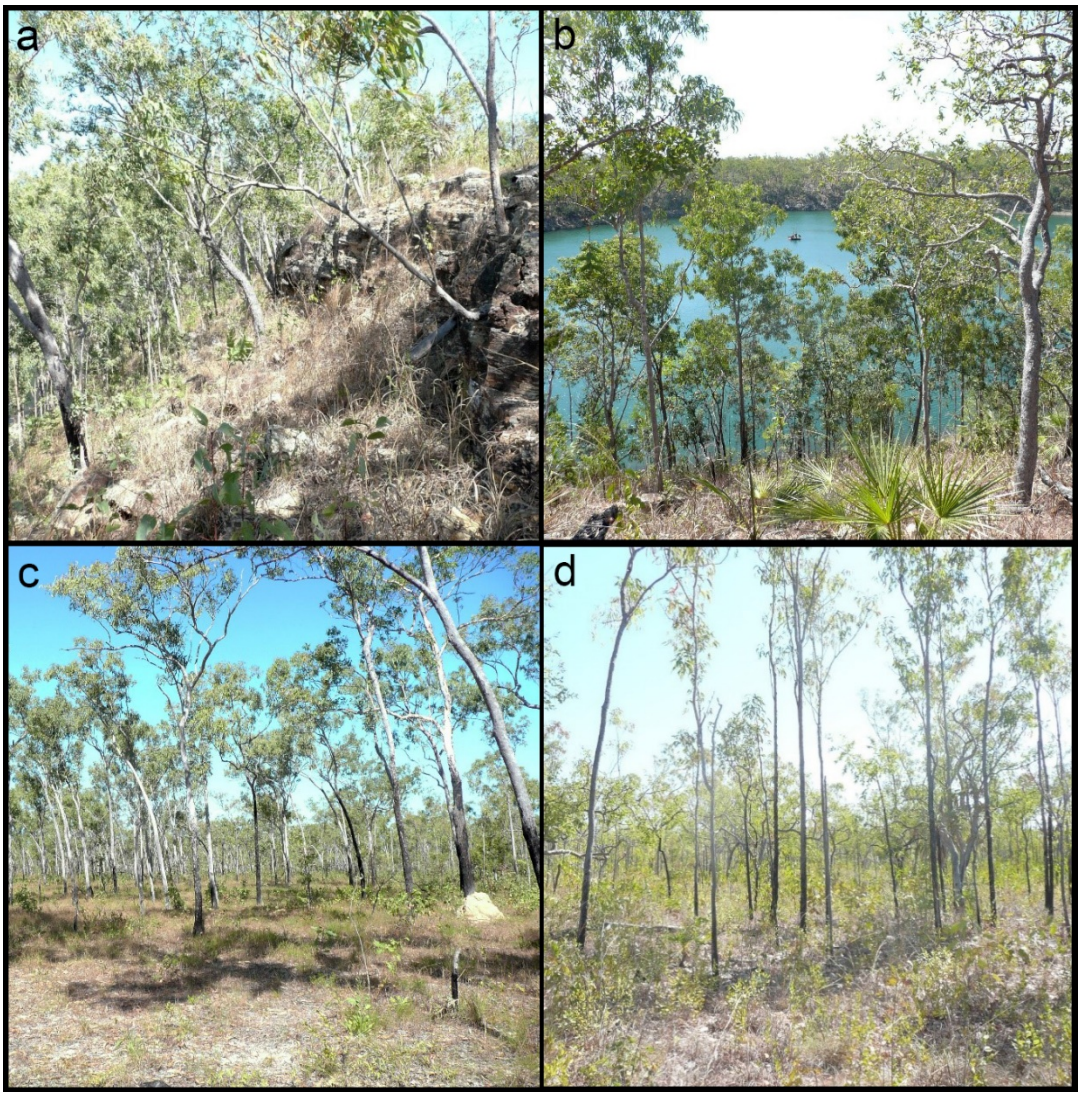

Figure 2: Vegetation at Marura: a) slope on the south to southwest edge, b) southeast edge looking northwest over the pool, c) northeast edge, and d) southern side of Marura.

In the 19 year period spanning 2000-2019 for which satellite data are available, the area (~10 km^2) surrounding Marura burned on average every 2 to 4 years (every year at its most frequent,

including the 2 km^2 containing the Marura sinkhole itself between 2008 and 2010) (Northern Australian Fire Information [NAFI] 2020). Fires in the period 2000-2018 were primarily between July and October, with three fire events in November (2001, <100 m from Marura; 2003, <1 km away; 2018, >3 km away) and two in December (2006, ~1 km away; 2019, <100 m away) (NAFI 2020). No recent fire events were evident at Marura during fieldwork in 2015, and the presence of *Callitris intratropica* also suggests a low-intensity fire regime and/or unburnt patches in the area as *C. intratropica* is known for its sensitivity to fire (see Bowman and Panton 1993; Trauernicht et al. 2015).

2.3 Archaeology and Land-Use History

Initial occupation of sites at Point Blane Peninsula in Blue Mud Bay has been dated to ~3000 BP (see Figure 1; Faulkner and Clarke 2004, p.28). Occupation has been divided by Faulkner (2013) into two distinct phases: 3000-1000 BP and 1000 BP to present. The first phase is characterised by "intense and focussed" sand and mudflat shellfish exploitation (Faulkner 2013, p.165). The transition between these phases marks a decline in exploitation of sand and mudflat shellfish species (Faulkner 2013). During the second phase, exploitation of mangrove species increases, and intensive site use shifts from Grindall Bay to Myaoola Bay (Faulkner 2013). Faulkner (2013, p.142) linked these observed shifts in human behaviour and site use to landscape changes (e.g. progradation and sedimentary infilling) and associated changes in resource availability.

Macassan *bêche-de-mer* (trepang) fishers from Sulawesi are known to have visited the Arnhem Land coast since the seventeenth century (Taçon et al. 2010), and Dutch voyages in the region are recorded in 1623 and 1644 without making landfall (Duyfken 1606 Replica Foundation 2016; Heeres 1899). European exploration of Arnhem Land increased in the nineteenth century

after British invasion of Australia (e.g. Flinders 1966).The first pastoral leases in the Northern Territory were granted in 1872 (National Archives of Australia 2018), with a lease of ~50,000 km² in Arnhem Land held by the Eastern and African Cold Storage Company in 1903 (Cole 1982). Six missions were established across Arnhem Land between 1908 and 1958, including at Rose River (now Numbulwar, see Figure 1) in the southeast and offshore on Groote Eylandt (McMillan 2008; Sydney Morning Herald 2004). Attempts at pastoralism were abandoned in the early twentieth century (McMillan 2008), and Groote Eylandt and Arnhem Land were declared Aboriginal Reserves in 1920 and 1931, respectively (National Museum of Australia 2018; Barrier Miner 1931; Sydney Morning Herald 2004). The nearest town to Marura is Numbulwar (~95 km to the south), with the largest population centre over 300 km away at Borroloola on the coast of the Gulf of Carpentaria. A road running east-west exists approximately 300 m north of Marura, with a north-south branch approximately 300 m east of the site, visible via satellite imagery and observed during fieldwork. A small track runs from the northern road to the northeast edge of Marura, accessed during fieldwork.

3. Methods

Samples were collected in the field in 2015. Sediment cores were collected in 1 m increments from a single coring location in the lake centre using a raft-mounted hydraulic corer modified from Eijkelkamp equipment. The total collected sediment depth was 5.85 m, beneath a water column of ~11 m. Cores were transported to James Cook University for refrigerated storage prior to sampling in the laboratory. Samples for this study were taken from the uppermost 3 m of sediment to focus on the late Holocene.

3.1 Radiometric dating

Samples were taken from the uppermost 26 cm of sediment in 1 cm increments for preparation for lead-210 dating by alpha spectrometry. Six 1 cm thick bulk sediment samples collected at regular intervals across the uppermost 3 m were prepared for radiocarbon dating by accelerator mass spectrometry. Lead-210 and radiocarbon sample preparation and analysis were undertaken at the Australian Nuclear Science and Technology Organisation (ANSTO).

Samples were prepared for lead-210 analysis by alpha spectrometry following the ANSTO Environmental Radioactivity Measurement Centre (ERMC) Lead-210 dating sample preparation method, as described in Supplementary Information (see also Eakins and Morrison 1978).

Bulk sediment samples for carbon-14 dating were pretreated using the ABA (Acid-Base-Acid) method prior to combustion to CO_2 using the sealed-tube technique. Samples were then converted to graphite by reduction with excess hydrogen over iron catalyst at 600°C to produce targets for AMS measurements (Hua et al. 2001). Carbon-14 accelerator mass spectrometry (AMS) measurements were performed on the STAR 2 MV particle accelerator at ANSTO Lucas Heights. Separate sub-samples of each fraction were combusted in a coupled elemental analyser-isotope ratio mass spectrometer system for measurement of $\delta^{13}C$ values, which were used to correct for fractionation (Fink et al. 2004).

Lead-210 (converted to calendar years BP, reported as years before 1950 CE) and radiocarbon dates (also calibrated to cal BP) were combined to form a Bayesian age-depth model using the *rBacon* package within *R* (see Blaauw et al. 2019; R Development Core Team 2013). Radiocarbon dates were calibrated to cal BP as part of this process within the *rBacon* package using the Southern Hemisphere calibration curve SHCal13 (Hogg et al. 2013).

3.2 Sediment Elemental Composition

Elemental analysis of core sediments was undertaken to provide context for the measured fire proxies. Sediment cores were scanned using an Itrax^{TM} µXRF core scanner at ANSTO. The core was scanned at 1000 µm intervals with 10 second exposure, using a molybdenum X-ray tube, to determine relative elemental composition. As the 3 m core was divided into 6 x 0.5 m segments for scanning, the lower 5 cm of measurements for each core segment were removed from the raw data prior to analysis to remove errors associated with transitions between segments. Itrax^{TM} elemental counts were normalized using the procedure outlined by Weltje et al. (2015); elements of interest were isolated after selection from interpreted elements listed by Davies, Lamb and Roberts (2015) and counts were normalized by dividing element counts by the incoherent scatter for that depth (see Weltje et al. 2015). Elemental data were averaged to 4 cm resolution for comparison to charcoal and pyrogenic carbon data during analysis, and principal components analysis was undertaken using R.

3.3 Charcoal

Sediment samples were prepared for optical charcoal analysis following the procedure outlined by Stevenson and Haberle (2005), in 1 cm intervals taken at 4 cm increments. Samples were soaked in ~5% hydrogen peroxide for approximately 72 hours to lighten organic matter. Samples were subsequently rinsed through nested sieves of 250 µm, 125 µm and 63 µm mesh. Water and sediment that passed through the 63 µm sieve were retained, with approximately 5 mL 37 % HCl added to ~500 ml supernatant to flocculate particles from suspension with excess

liquid poured off. The <63 µm size fraction was retained to process for pyrogenic carbon by hydrogen pyrolysis (see below).

Samples in three size fractions (>250 µm, 250-125 µm and 125-63 µm) were analysed under a stereomicroscope (x20 magnification) while suspended in water. Charcoal particles were counted and categorised by morphology using the system developed by Enache and Cumming (2006). Charcoal particles >125 µm are interpreted in this study as local, with particles <125 µm interpreted as derived from the broader regional environment; it is not possible to specify source areas with certainty due to ongoing debate regarding the potential for long-distance transport of particles (see Vachula et al. 2018 for discussion). Charcoal count data were converted to charcoal accumulation rates (influx, particles cm^{-2} y^{-1}) using recorded sample volume and mean age derived from the Bayesian age-depth model using the *rBacon* package. Width-length measurements were recorded for charcoal particles in the macroscopic size fractions (>125 µm). Following Aleman et al. (2013) and Leys, Commerford and McLauchlan (2017), particles with an aspect ratio of <0.5 or greater were categorised as "elongate" and indicative of grass, with particles of aspect ratios of 0.5 or greater categorised as non-elongate and thus derived from non-grass fuels such as leaves or wood.

3.4 Hydrogen Pyrolysis and Stable Carbon Isotopes

Pyrogenic carbon analysis via hydrogen pyrolysis was included as a distinct but complementary fire proxy to charcoal, representative of resistant products of biomass burning (Wurster et al. 2012). Bulk sediment samples and the <63 µm fraction isolated during charcoal sample preparation were both prepared for hydrogen pyrolysis. Samples were dried and homogenized before being loaded with a Mo catalyst (approximately 10% sample weight) using an aqueous/methanol solution of ammonium dioxydithiomolybdate [$(NH_4)_2MoO_2S_2$]

(Ascough et al. 2009; Wurster et al. 2012). Dried catalyst-loaded samples were transferred to glass inserts and loaded into the reactor of the hydrogen pyrolysis rig in the Advanced Analytical Centre at James Cook University, Cairns. Samples were pressurised with 15 MPa of hydrogen with a sweep gas flow of 5 L min^{-1} and then heated at 300°C min^{-1} to 250°C before heating more slowly at 8°C min^{-1} to a final hold temperature of 550°C for 2 mins (Wurster et al. 2012).

Sample carbon content and carbon isotope composition ($\delta^{13}C$) before and after hydrogen pyrolysis were measured using a Costech Elemental Analyser fitted with a zero-blank auto-sampler coupled via a ConFloIV to a ThermoFinnigan $DeltaV^{PLUS}$ using continuous flow isotope ratio mass spectrometer (EA-IRMS). Percent pyrogenic carbon for each sample was calculated from percent carbon of hydrogen pyrolysis residue divided by total organic carbon of the sample. Percent pyrogenic carbon was converted to pyrogenic carbon accumulation rates (influx, g cm^{-2} y^{-1}) using recorded bulk density and mean age derived from the Bayesian age-depth model developed using the *rBacon* package. Pearson's correlation was undertaken in R for charcoal and pyrogenic carbon influxes. Stable carbon isotope results are reported relative to Vienna Peedee belemnite (VPDB), and precision (SD) with internal standards was better than ±0.1‰. Isotopic composition of the pyrogenic (black) carbon, of both the bulk and <63 µm fraction, was calculated in R using the equation given in Wurster et al. (2012). $\delta^{13}C$ values of ~-27‰ or less are associated with C_3 plants (trees and woody vegetation) while ~-12‰ or more is indicative of C_4 plants (grasses), with values between these end members reflecting mixed C_3/C_4 composition (O'Leary 1988; Saiz et al. 2018; Wurster et al. 2012).

4. Results

4.1 Chronology

Lead-210 and radiocarbon dates are presented in the Supplementary Material (Tables S1 and S2). The Bayesian age-depth model for Marura shows a relatively steady accumulation rate throughout the record (Figure 3). While samples above 10 cm depth (0-1, 4-5 and 8-9 cm) are assigned ages (-50, -35 and -20 cal BP, respectively) within the age-depth model, lead-210 analysis suggests mixing across these depths with all three samples representing conditions since ~1950 CE (0 cal BP).

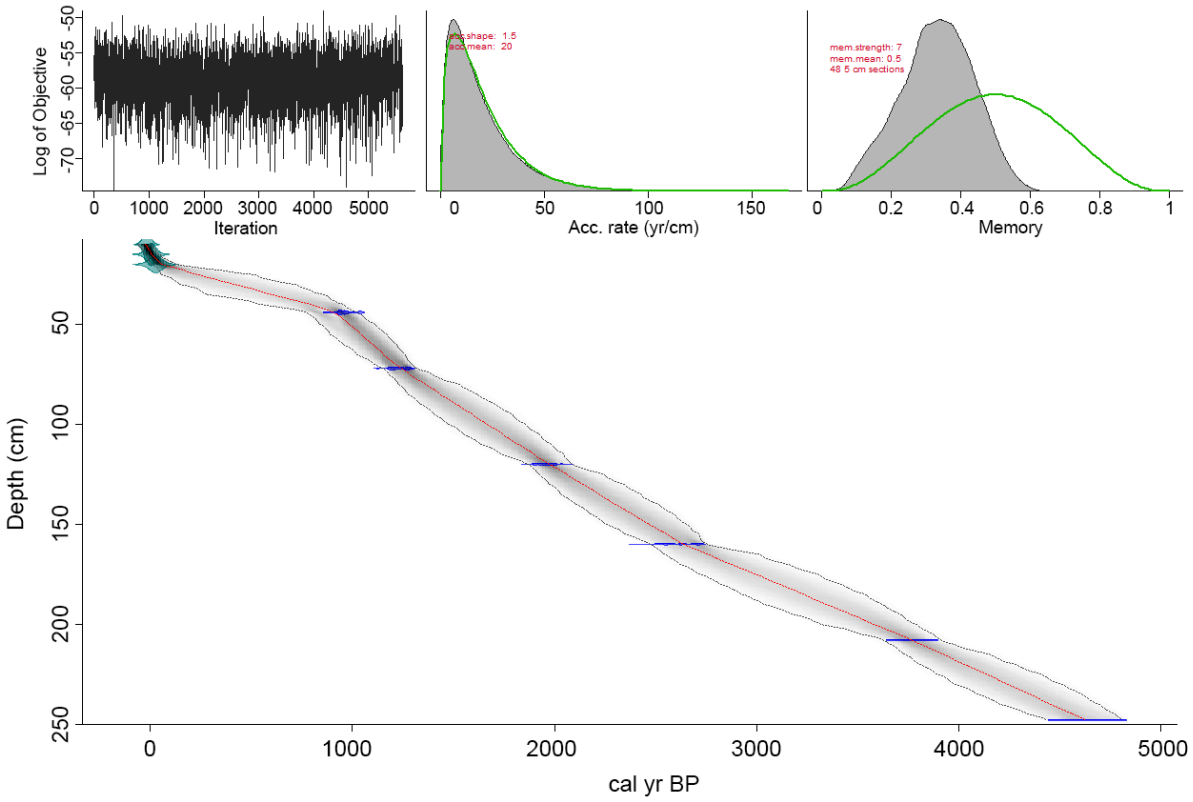

Figure 3: Age-depth model for Marura (MAR2), with lead-210 dates indicated in green and radiocarbon dates in blue.

4.2 Elemental Composition

Elements of interest in the Marura record include Ti, Fe and Rb as these elements are commonly interpreted as deriving from detrital sources (Davies, Lamb and Roberts 2015). An organic signal, represented by Mo inc/Mo coh (Mo ratio; Woodward and Gadd 2019), dominates for most of the record except for a more detrital phase between ~75 cm and 110 cm depth (Figure 4). Strong positive correlations are present between magnetic susceptibility (MS) and all selected elements of interest ($r^2 > 0.5$).

MS and all elements of interest cluster along the x axis in a Principal Components Analysis (Figure 4b). This axis represents principal component 1, explaining ~62.7 % of variance and representing organic input (Mo ratio) versus detrital input (MS and all other elements).

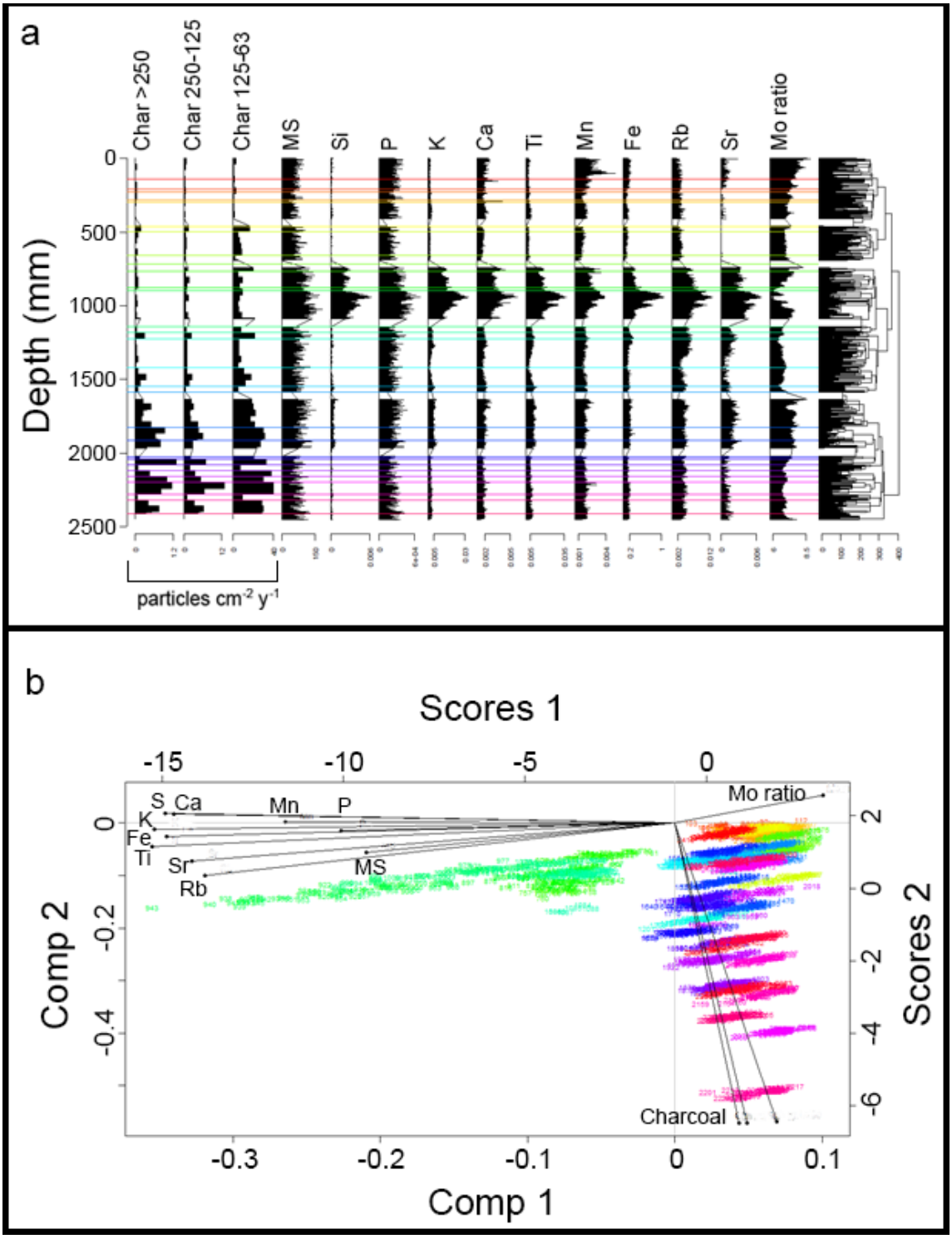

Figure 4: Itrax™ XRF elemental composition for Marura 0-2.9 m: a) stratigraphic plot, b) Principal Components Analysis. Coloured numbers (sample depths) in plot b correspond to coloured depth zones identified by clustering in plot a.

Strong positive correlations ($r^2 > 0.85$) exist between all three size charcoal influxes. Charcoal influx variables have weak correlations to all other variables ($r^2 < \pm 0.25$). <63 µm pyrogenic carbon influx is also strongly correlated with charcoal influxes ($r^2 > 0.74$), while bulk pyrogenic carbon influx is weakly positively correlated to <63 µm pyrogenic carbon influx and charcoal influxes ($r^2 < 0.35$). Charcoal and pyrogenic carbon influxes cluster in the lower right quadrant of Figure 4b, and are separated from all other variables along the y axis representing principal component 2 (~19.8% of variance).

4.3 Charcoal

Charcoal influx (particles cm^{-2} y^{-1}) is highest early in the record for all size fractions, declining through time (Figure 5). The highest influxes in all size fractions occur between the beginning of the record (~4600 cal BP) and 2800 cal BP. Influxes in the macroscopic (>125 µm) size fractions noticeably decline after 2800 cal BP, while the 125-63 µm fraction declines less sharply after this point. The lowest charcoal influx values in the record occur in the most recent period, from ~800 cal BP to the present, with a slight increase in influx in the last century.

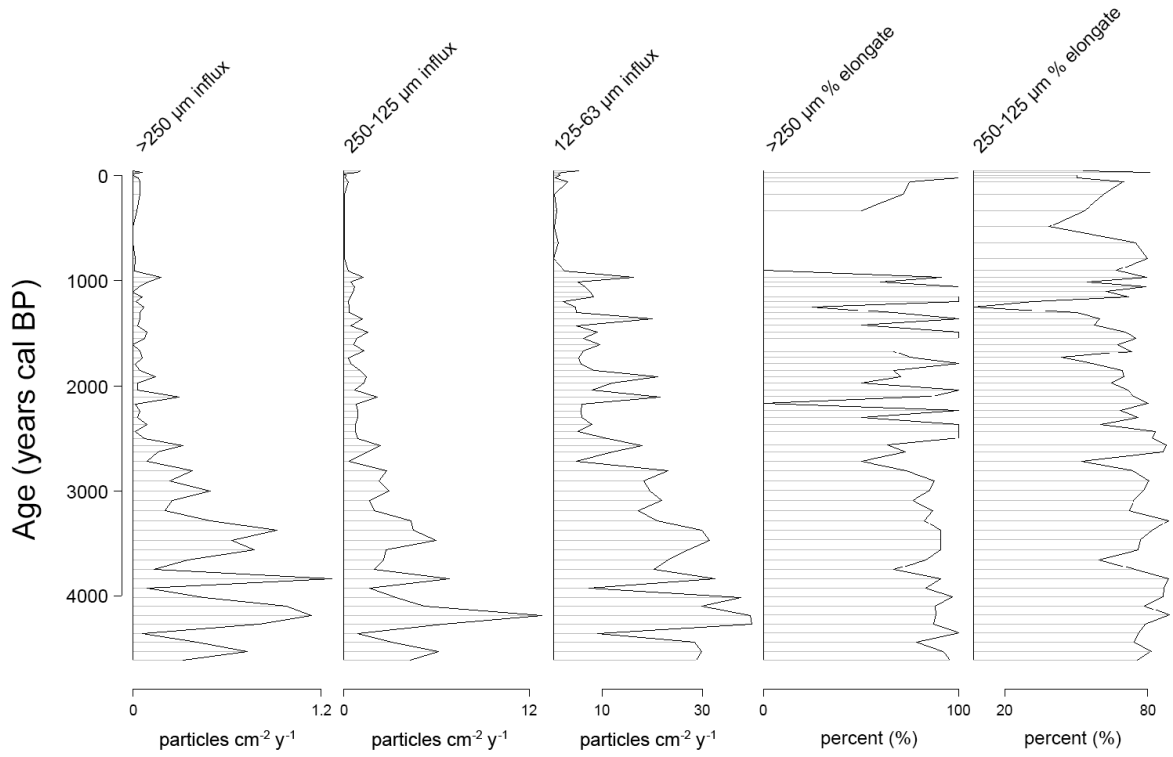

Figure 5: Charcoal fluxes and elongate particle percentages from aspect ratios.

Elongate charcoal particles as determined from aspect ratios are present throughout the record, with high percentages of elongate particles in samples in the lower half of the record, increasing in variability in the upper half of the record into the present. This increasing variability (primarily visible as sharp peaks and troughs) coincides with decreasing total charcoal abundance and may therefore be the result of low sample sizes. However, declining elongate particle percentages determined by morphotypes also occur in the 250-125 µm and 125-63 µm size fractions. Morphotype data is presented in the Supplementary Material (Figures S1, S2 and S3).

4.4 Pyrogenic Carbon and Isotopic Composition

Pyrogenic carbon influxes (g cm^{-2} y^{-1}) in the bulk and <63 µm fractions show declining trends through time comparable to charcoal influxes (Figure 6). Peak timing, however, varies between charcoal influxes and both pyrogenic carbon influxes are indicative of varying relative fire intensities. Pyrogenic carbon influx in the <63 µm fraction is strongly correlated with 125-63 µm charcoal influx ($r^2 = 0.71$).

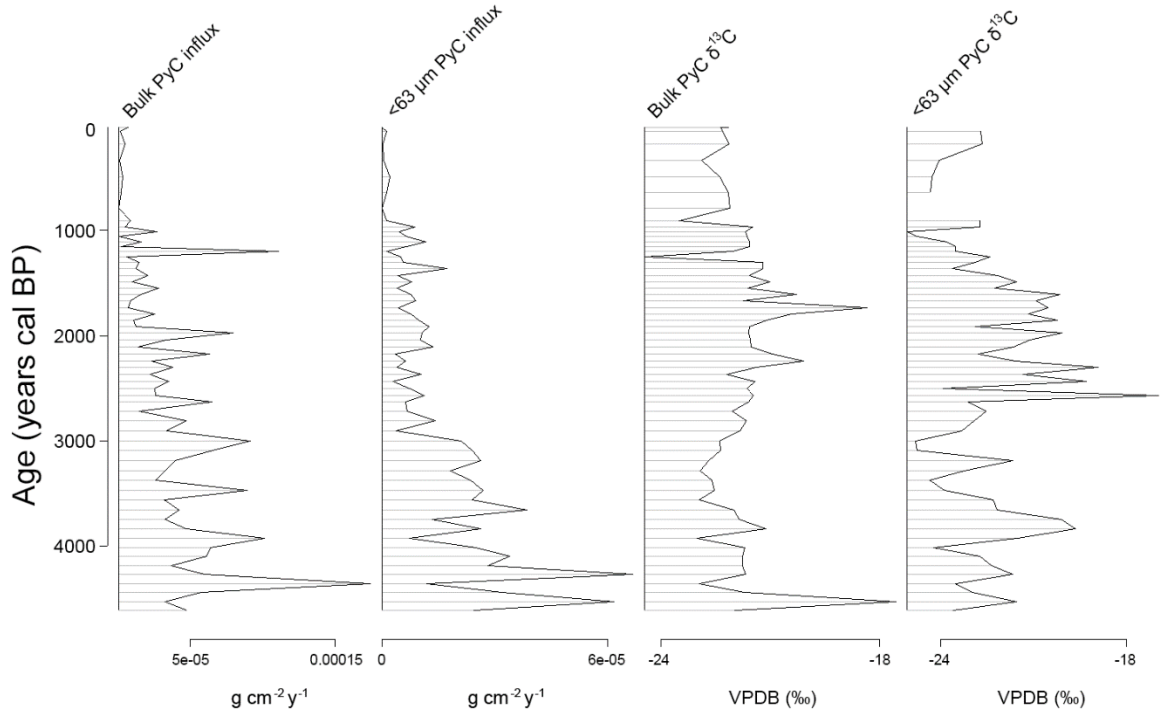

Figure 6: Pyrogenic carbon flux and $\delta^{13}C$ values for bulk and <63 µm fractions.

Pyrogenic carbon $\delta^{13}C$ values in the bulk sediment vary between -18 and -24 ‰, while values in the <63 µm size fraction vary over a slightly wider range between -17 and -25 ‰. While no overall trend is apparent for bulk pyrogenic carbon $\delta^{13}C$ values, trends may be present in the

<63 µm size fraction. $\delta^{13}C$ values in this fraction are consistently higher (less ^{13}C-depleted) from ~2600-1500 cal BP, with periods of lower $\delta^{13}C$ values before and after this, except for a brief increase from ~3900-3600 cal BP.

4.5 Relative Fire Intensity: Charcoal and Pyrogenic Carbon

As the pyrogenic carbon content of charcoal increases with increasing temperature (see Bird and Ascough 2012), the combination of charcoal and pyrogenic carbon influx data allows for the qualitative identification of periods or trends associated with different relative fire intensities. Influx data for pyrogenic carbon and total charcoal particles were converted to Z scores to evaluate relative fire intensity (Figure 7). High intensity periods were identified, characterised by high pyrogenic carbon Z scores and frequently associated with low total charcoal particle Z scores (due to charred biomass being substantially converted to pyrogenic carbon measurable by hydrogen pyrolysis).

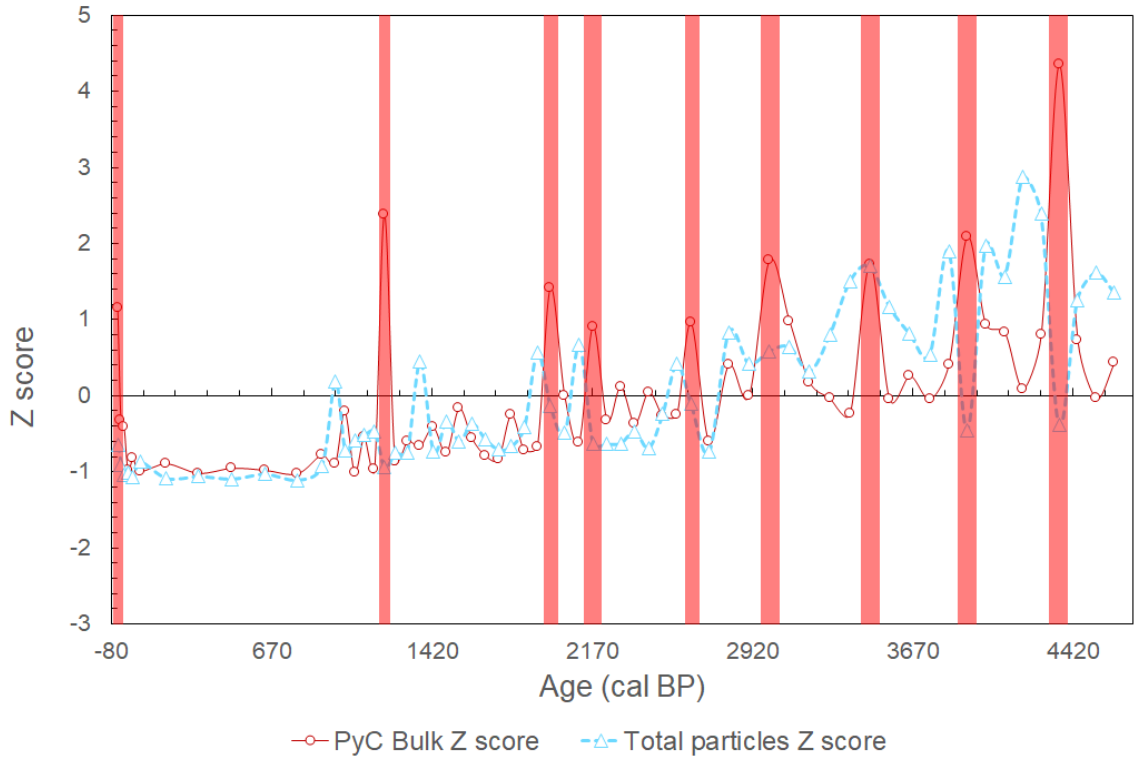

Figure 7: Z scores of pyrogenic carbon influx (red line, circle markers) and total charcoal particle influx (blue dashed line, triangle markers). High relative fire intensities (red bars) are identified by positive pyrogenic carbon Z scores and low to negative total charcoal Z scores.

High intensity periods occur at approximately 450-year intervals early in the record. These intervals become irregular after the high intensity peak at 3000 cal BP. Pyrogenic carbon and charcoal influxes remain low for most of the last 900 years of the Marura record, with a high intensity peak in the uppermost sample (0-1 cm).

5. Discussion

5.1 Relative Fire Intensity

Fire intensity can be broadly defined as the rate of energy release from a fire and incorporates temperature and residence time, while fire severity refers to "the loss or decomposition of organic matter" and ecosystem responses to fire (Keeley 2009, p.119). Fire intensity has been linked to seasonality, with experimental fire studies in northern Australian savannas recording low fire intensities for burns occurring in the early dry season (from the cessation of rain until July) compared to higher intensities for late dry season burns when fuels are drier and fire weather may be more extreme (August onwards) (Williams, Gill and Moore 1998; Russell-Smith and Yates 2007). Trauernicht et al. (2015, p.1914) suggest that fire intensity and heterogeneity are affected by human fire management while the total extent of landscape burnt is primarily driven by climate. This is due to anthropogenic fire regimes potentially altering seasonality and patchiness (size of individual burns) but not affecting the amount of fuel available to burn or overall fire frequency (e.g. Hoffmann et al. 2002, p.4). Indigenous Australian fire regimes in northern Australia are associated with burns throughout the dry season (Crowley and Garnett 2000; Preece 2002; Bowman, Walsh and Prior 2004) while unmanaged or uninhabited landscapes in this region typically burn in the late dry season (Yibarbuk et al. 2001; Russell-Smith et al. 2003; Bowman, Walsh and Prior 2004). If traditional measures of biomass burning (e.g. charcoal influx) are primarily capturing information on total area burned (e.g. Leys et al. 2015), these measures will be sensitive to climate signals but unable to detect an anthropogenic signal within a fire record (Trauernicht et al. 2015). Fire intensity data are therefore critical in separating potential climatic and anthropogenic influences within a palaeofire record.

Relative fire intensity in the Marura record is variable, displaying a mix of periods of high and intermediate to low fire intensities. If variation in fire intensity is taken as an indicator of

anthropogenic influence (following Trauernicht et al. 2015), the Marura record indicates significant levels of human influence on landscape fire at some times. The absence of anthropogenic burning in the tropical savannas of northern Australia has been associated with large scale, high intensity "wildfires" in the late dry season, with a fire return interval of 1-3 years (Yibarbuk et al. 2001, p.329, 337); the presence of substantial periods of cool, low intensity fires in a palaeofire record therefore may also suggest human intervention through low intensity burns lit throughout the dry season. As these management burns are frequently associated with smaller fires (e.g. Yibarbuk et al. 2001; Russell-Smith and Yates 2007; Trauernicht et al. 2015), this influence may also be discernible from charcoal size fraction data.

5.2 Fire History

5.2.1 Phase I: 4600 to 2800 cal BP

All charcoal and pyrogenic carbon influxes are highest during this phase, peaking around 4300-4000 cal BP (Figure 8). An organic-rich period of sedimentation also begins during this phase (~4000 cal BP), identified by total organic carbon content and Itrax^{TM} µXRF (see Figure 4). Pyrogenic carbon $\delta^{13}C$ values in this phase show mixed C_3/C_4 contribution (-18 to -23‰ for bulk and -20 to -25‰ for the <63 µm fraction), and elongate charcoal particle contributions show very similar trends across all size fractions (from 59.6 to 100% from aspect ratios, and 12 to 69% from morphotypes), suggesting similarities in tree-grass ratio across spatial scales within and beyond the catchment of Marura. However, differing influxes and estimated grass contributions across size fractions after the early part of the record suggest fires were not simultaneously affecting within and beyond the Marura catchment. Bulk and <63 µm pyrogenic carbon $\delta^{13}C$ values display matching trends for the uppermost samples in this phase; a peak (-18‰) at ~4500 cal BP indicates high grass contribution to the pyrogenic carbon under

intermediate/indeterminate fire intensity conditions, followed shortly after by a trough at ~4350 cal BP (-24‰) indicating high woody content under high fire intensities, with most grass biomass completely combusted. After this time, bulk and <63 µm $\delta^{13}C$ values change independently, suggesting that C_3/C_4 vegetation compositions were similar in the Marura catchment and greater region at the beginning of this phase but diverged after this point. Fire intensities are mixed during Phase I as both charcoal and pyrogenic carbon fluxes are high throughout this phase, with high intensity periods occurring approximately every 450 years.

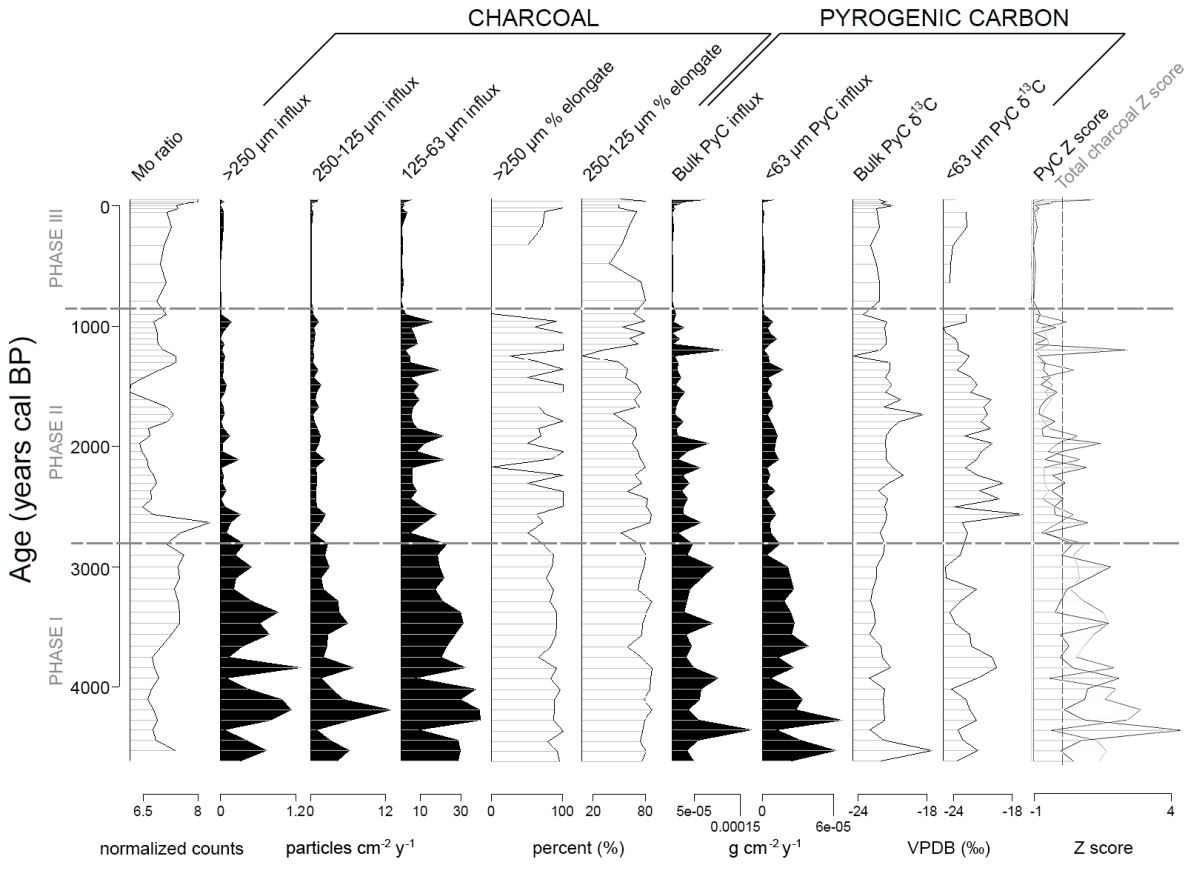

Figure 8: Combined data from previous figures including Mo ratio from Itrax™ µXRF, charcoal fluxes and percent elongate particles, pyrogenic carbon fluxes and $\delta^{13}C$ values, and Z scores (pyrogenic carbon in black, total charcoal in grey) presented in Figure 7.

Multiple palaeoenvironmental records from central and western northern Australia show a drying trend into the late Holocene coinciding with Marura Phase I. The onset of this drying trend ranges from ~4 ka (Kapalga South Billabong; Shulmeister and Lees 1995) to ~3 ka (Black Springs; McGowan et al. 2012). Shulmeister (1992) identifies a precipitation maximum at ~4 ka for Four Mile Billabong on Groote Eylandt followed by a precipitation decline from ~3.8 ka. Biomass promoted by the mid-Holocene precipitation maximum likely provided fuel for increased fire incidence during the transition to increasingly dry and variable conditions in the late Holocene (e.g. Prebble et al. 2005). Peak charcoal and pyrogenic carbon influxes at Marura (~4000 cal BP) coincide with this regional transition from higher effective precipitation in the mid-Holocene to drier and/or more variable conditions into the late Holocene suggesting a climatic control on fire incidence and mixed composition of C_3 and C_4 burning in this phase.

5.2.2 Phase II: 2800 to 900 cal BP

While charcoal and PyC influxes all show a decreasing trend throughout the Marura record, the most pronounced change in influx occurs around 2800 cal BP. After 2800 cal BP, all influx values are lower than the maximum values seen in Phase I; only a single peak in bulk pyrogenic carbon influx (indicating a high intensity fire event) at ~1200 cal BP reaches comparable levels to values in Phase I. This decrease in influx is most apparent in the macroscopic charcoal size fractions. Additionally, elongate particle contributions to the largest macroscopic charcoal size fraction (>250 μm) increase in variability at this time and no longer show similar trends to elongate particles in the other size fractions. Despite this, charcoal influxes for all size fractions are most strongly correlated during this phase. High fire intensities are not evenly distributed during Phase II, and several charcoal peaks occur at lower levels than those seen in Phase I. In

Phase II (~2600 cal BP), the Marura XRF record ceases to be dominated by an organic elemental signal. A minor peak in detrital elements occurs in this phase from ~1900 to ~1300 cal BP, along with a trough in total organic carbon percentages; this does not appear to correspond to any other proxies measured in this study.

Phase II is difficult to classify at a regional scale as many sites show increasing climate variability, often linked to variations in the Indonesian-Australian Summer Monsoon or intensification of ENSO, expressed in different ways. For example, Field et al. (2017, p.14) described short alternating wet and dry periods from 5000-2600 cal BP at Black Springs (in the northern Kimberley) followed by "pronounced" aridity until ~1300 cal BP then a transition to "modern conditions". Similarly, Rowe et al. (2019, p.25) showed wetland contractions at Girraween Lagoon (near Darwin) at ~2850 and 1300-1250 cal BP. Head and Fullager (1992, p.29) described "less fluctuation in water levels in the last 1 – 2,000 years than previously" at swamp sites in the west of the Northern Territory and contrast this to concurrent periods of aridity inferred from dune instability at Cape Flattery on Cape York Peninsula (Queensland) and the Berkeley River in the Kimberley (Western Australia). Shulmeister and Lees (1995, p.12) also noted three phases of dune activation during this period, as well as a "sharp decline" in effective precipitation at Groote Eylandt from 3700-1000 BP with increasing precipitation thereafter.

During this period, archaeological data become available in the Blue Mud Bay area. Marura Phase II corresponds broadly to the first occupation phase of Point Blane Peninsula outlined by Faulkner (2013) of focused sand and mudflat shellfish exploitation from 3000-1000 BP.

While climate is likely the dominant driver of fire during Phase I, anthropogenic burning becomes increasingly important from Phase II onwards. Lower overall fire incidence compared to Phase I is likely due to continuing dry conditions producing less biomass than during the

mid-Holocene precipitation maximum. Variable fire intensities with irregular intervals between high intensity periods, a declining trend in fire incidence throughout Phase II, and consistently low levels of macroscopic charcoal influx suggestive of restricted burned areas indicate that Marura was likely actively managed during this time. This is particularly evident after ~1900 cal BP with the reduction of high intensity burns (and a reduction of bulk pyrogenic carbon influx overall) exception for a high intensity event at ~1200 cal BP.

While both bulk and <63 μm pyrogenic carbon $\delta^{13}C$ values show a mixed C_3/C_4 contribution throughout the Marura record, these size fractions behave differently, with much higher variability in the <63 μm size fraction that is particularly noticeable during this phase and is interpreted as indicating landscape changes beyond the Marura catchment. Phase II also shows more variability in bulk pyrogenic carbon $\delta^{13}C$ values than the preceding phase (not including dramatic deviations near the beginning of Phase I, discussed above); however, low and high intensity phases of burning do not affect bulk pyrogenic carbon $\delta^{13}C$ values as directly or noticeably as in the previous phase.

Through indications such as short, alternating fire intensity phases and decoupling of bulk pyrogenic carbon $\delta^{13}C$ values from fire intensity changes, the fire record in Phase II is considered to be human-driven. This style of burning, as active fire management, is well documented; multiple studies by Bliege Bird et al. (2008, 2012, 2013) described mosaic burning for subsistence in the Western Desert creating landscape patchiness, functioning as a buffer to climate-driven large scale fires and promoting species such as varanid lizards that require both burnt and unburnt habitat patches. Russell-Smith et al. (1997) detailed similar methods of burning for resource management in western Arnhem Land, and these methods are now utilised by over 70 registered savanna burning projects across northern Australia (Ansell et al. 2019).

Trauernicht et al. (2015, p.1912) demonstrated the effects of patch burning in the savannas of Arnhem Land by mapping the modern distribution of the fire-sensitive conifer *Callitris intratropica*, concluding that small fires increase patch ages, patch age diversity and fire-return intervals compared to "fewer, larger fires burning the same proportion of the landscape". The mixed C_3/C_4 contribution in Phase II is therefore suggested to reflect a reorganised spatial arrangement of tree-grass vegetation within the Marura catchment. The reduction of elongate charcoal particles after ~2300 cal BP may reflect anthropogenic burning aimed to increase woody plant diversity at the expense of grasses, as described by Rowe et al. (2019, p.27) at Girraween Lagoon near Darwin, with peak *Eucalyptus* contribution at Girraween Lagoon from 2850-600 cal BP.

The return to a dominant organic signal at Marura towards the end of this phase (~1000 cal BP) corresponds to the effective precipitation "recovery" at ~1000 cal BP described by Shulmeister (1992, p.113) at Four Mile Billabong (Groote Eylandt). This suggests the latest peaks in charcoal and pyrogenic carbon influx at the end of Phase II were fuelled by an increase in biomass enabled by improved effective precipitation, under low intensities similar to the increase in "'cool' fires" after ~1000 cal BP at Four Mile Billabong (Shulmeister 1992, p.112).

5.2.3 Phase III: 900 cal BP to Present

Charcoal and pyrogenic carbon influxes drop to their lowest levels for all sizes in the Marura record after ~900 cal BP, and total organic carbon percentages and the XRF elemental record reflect high organics for the remainder of the record. Phase III contains the weakest correlations between the >250 µm charcoal size fraction and other sizes, with many samples containing no charcoal measuring >250 µm, while the relationship between the 250-125 µm and 125-63 µm fractions remains strong ($r^2 = 0.81$). This suggests connectivity between burning at local and

regional scales, but potentially limited fire occurrence close to the edges of Marura. Minimal variation in $\delta^{13}C$ values for both bulk (-21 to -23 ‰) and <63 μm (-23 to -24 ‰) pyrogenic carbon occurs after this point in the record.

Marura Phase III corresponds to the second main occupation phase of Point Blane Peninsula, associated with a decline in the exploitation of sand and mudflat shellfish at ~1000 BP and increase in the exploitation of mangrove species after ~500 BP at Myaoola Bay (Faulkner 2013, p.141, 170). Humans were therefore mobile around the Blue Mud Bay region during this period, actively adapting to changing resource availability. From this, it is proposed that human use of Marura and the surrounding landscape continued through this period, with an increase in mobility.

Low charcoal and pyrogenic carbon influxes during this phase likely reflect a decrease in the effective transport of these fire products into the site due to fine scale landscape patchiness developed and maintained by anthropogenic burning. This patchiness reduced the capacity of rain events to transport larger pyrogenic carbon particles overland into the lake.

Charcoal and pyrogenic carbon influxes show an increase at the very end of this phase, after 55 cal BP. Influxes for every size fraction (except for >250 μm) peak in the uppermost sample (MAR2 0-1 m 0-1 cm) to values not seen since the end of Phase II. As this occurs within the potentially mixed uppermost 10 cm of sediment, the timing and exact nature of this increase is uncertain as influx measures incorporate the age of a sample; however, an increase in the uppermost 8 cm is also visible when measured as charcoal concentration (particles/cm^3). Interestingly, <63 μm pyrogenic carbon influx also displays a minor peak between ~650 and ~450 cal BP, reflected in a peak at ~640 cal BP in 125-63 μm charcoal influx but otherwise not discernible in other size fractions suggesting a strictly regional increase of intermediate intensity fire not visible in the local signal.

Arnhem Land was under pastoral lease from the late 19th to early 20th centuries, before the establishment of the Arnhem Land Aboriginal Reserve in 1931 (Barrier Miner 1931; Cole 1982). Russell-Smith et al. (1997, p.180) noted the prevalence of intense late dry season fires in western Arnhem Land beginning in the last century with the "collapse of traditional management practice", with such fires becoming commonplace after the 1940s. Changes in settlement patterns also led to altered fire management in areas such as Arnhem Land even after management was returned to traditional owners (see Head 1994, p.177). This is potentially reflected by high bulk pyrogenic carbon influx in the most recent samples from Marura, suggesting high fire intensities as associated with European-influenced or unmanaged late dry season burns; however, lead-210 dating results suggest mixing in the uppermost 10 cm of sediment and therefore no definitive conclusions can be drawn regarding the most recent period within the Marura record.

5.3 Anthropogenic influence

The Marura palaeofire record displays a combination of climate and anthropogenic effects on fire, with the role of human-driven fire regimes becoming increasingly important over time. The dominant climate driver in this region throughout the Holocene is the Indonesian-Australian Summer Monsoon and past periods of increased and decreased effective precipitation in northern Australia have been associated with movement of the Intertropical Convergence Zone (ITCZ) southwards and northwards, respectively (e.g. Reeves et al. 2013). Multiple records across northern Australia show an effective precipitation maximum in the early to mid-Holocene (Shulmeister 1992; Nott and Price 1994; Shulmeister 1999; Denniston et al. 2013; Field et al. 2017; Rowe et al. 2019). The mid-to-late Holocene transition is associated with declining effective precipitation (e.g. Shulmeister 1992; Rowe et al. 2019),

described by Denniston et al. (2013, p.163) as a “dramatic and sustained weakening of monsoon rainfall” at KNI-51 in the eastern Kimberley. The late Holocene is frequently characterised as “increasingly variable” (Reeves et al. 2013, p.110) associated with weakening of the Indonesian-Australian Summer Monsoon (Shulmeister 1992; Denniston et al. 2013; Field et al. 2017; Rowe et al. 2019).

Charcoal and pyrogenic carbon influxes at Marura are highest at the mid-to-late Holocene transition period (early Phase I), associated with high effective precipitation in the region. High fire incidence in Phase I was therefore likely fuelled by abundant tree-grass biomass produced under conditions of initially high, and subsequently declining, effective precipitation. High fire intensities occur at ~450-year intervals in Phase I and it is difficult to discern possible anthropogenic influence during this period, particularly as archaeological evidence is also lacking for this phase. Relative fire intensities become variable in Phase II (2800-900 cal BP), coincident with the first occupation phase at nearby Blue Mud Bay (Faulkner 2013). While climate-driven fire in Phase I supported regional homogeneity of vegetation structures linked to dominant fire intensities, anthropogenic burning in Phases II and III promoted mixed and spatially variable C_3/C_4 vegetation within and beyond the catchment.

Decreasing charcoal and pyrogenic carbon influxes through these phases may have resulted from the establishment of patch-scale burning (see Bliege Bird et al. 2008; Bliege Bird, Bird and Codding 2016; Gammage 2012) across the Blue Mud Bay landscape potentially minimising or restricting the transport of charcoal and pyrogenic carbon into the sinkhole from more distant fires, combined with variable rainfall restricting available biomass. Peaks across charcoal and pyrogenic carbon influxes over the last 100 years to levels not seen since ~900 cal BP may coincide with the cessation of traditional indigenous burning practices in the area

(e.g. Haberle 2005; Moss et al. 2015) although sediment mixing is likely in the uppermost 10 cm of this record.

6. Conclusion

The multiproxy record presented in this paper enables new insights into the fire history of Arnhem Land, which to date has been underrepresented in palaeoecological research. The late Holocene record at Marura reflects the influence of both climate and humans on landscape fire in the tropical savanna of eastern Arnhem Land. Fire incidence was at its peak at Marura from the mid-to-late Holocene transition (~4600-2800 cal BP), coincident with higher effective precipitation regionally, and declined toward the present as weakening of the monsoon reduced effective precipitation and increased rainfall variability. Humans replaced climate as the main driver of fire at Marura after ~2800 cal BP, corresponding with archaeological evidence of occupation of Blue Mud Bay, applying varying fire intensities to support heterogeneous patches of mixed C_3/C_4 vegetation..

This record demonstrates the enhanced interpretive power of a multiproxy approach to fire reconstruction. Determining fire intensity is critical to distinguishing anthropogenic effects on fire from the influence of climate, achieved in this study through the novel combination of charcoal and pyrogenic carbon analyses. This composite technique is applicable to environments outside of the tropics and will improve future attempts to disentangle anthropogenic influence from other drivers in fire reconstructions.

Data Availability

The data presented in this paper are available within the following dataset:

Rehn, E. (2019): PhD Dataset: Fire and Environmental Change in Northern Australian Savannas during the Holocene. James Cook University. (dataset). http://doi.org/10.25903/5de5f1e48e86d.

Author Contributions (CRediT Statement)

Conceptualization, E.R., C.R., S.U., C.W. and M.B.; methodology, E.R., C.R., C.W. and M.B.; formal analysis, E.R.; investigation, E.R.; resources, C.R., C.W. and M.B.; writing—original draft preparation, E.R.; writing—review and editing, E.R., C.R., S.U., C.W. and M.B.; visualization, E.R..; supervision, C.R., S.U., C.W. and M.B.; project administration, M.B.; funding acquisition, E.R. and M.B.

Acknowledgements

This project was undertaken with the support of an Australian Research Council Laureate Fellowship to MIB (FL140100044) and the Australian Research Council Centre of Excellence for Australian Biodiversity and Heritage (CE170100015). ER acknowledges financial support from the Australian Institute of Nuclear Science and Engineering (Postgraduate Research Award 12143). The authors would like to thank Michael Brand, Rainy Comley, Dr Jordahna Haig, Dr Jennifer Whan, Dr Chris Wurster and Costjin Zwart for assistance during fieldwork and laboratory analyses at James Cook University, and Patricia Gadd, Dr Geraldine Jacobsen, Sabika Maizma and Atun Zawadzki for laboratory assistance at the Australian Nuclear Science

and Technology Organisation. We thank the two anonymous reviewers for their time in providing valuable feedback on the manuscript.

References

Aleman, JC, Blarquez, O, Bentaleb, I, Bonté, P, Brossier, B, Carcaillet, C, Gond, V, Gourlet-Fleury, S, Kpolita, A, Lefèvre, I, Oslisly, R, Power, MJ, Yongo, O, Bremond L and Favier, C (2013) Tracking land-cover changes with sedimentary charcoal in the Afrotropics. *The Holocene* 23(12): 1853-1862.

Andersen, AN, Cook, GD and Williams, RJ (2003) *Fire in Tropical Savannas*. New York: Springer-Verlag.

Ansell, J, Evans, J, Adjumarllarl Rangers, Arafura Swamp Rangers, Djelk Rangers, Jawoyn Rangers, Mimal Rangers, Numbulwar Numburindi Rangers, Warddeken Rangers, Yarrkala Rangers and Yugul Mangi Rangers (2019) Contemporary Aboriginal savanna burning projects in Arnhem Land: A regional description and analysis of the fire management aspirations of Traditional Owners. *International Journal of Wildland Fire*: article no. WF18152.

Ascough, PL, Bird, MI, Brock, F, Higham, TFG, Meredith, W, Snape SE and Vane, CH (2009) Hydropyrolysis as a new tool for radiocarbon pre-treatment and the quantification of black carbon. *Quaternary Geochronology* 4: 140-147.

Barrier Miner (1931) Arnhem Land: Proposal to declare Aboriginal Reserve. *Barrier Miner*, 4 September, 1.

Bird, MI and Ascough, PL (2012) Isotopes in pyrogenic carbon: A review. *Organic Geochemistry* 42: 1529-1539.

Bird, MI, Brand, M, Diefendorf, AF, Haig, JL, Hutley, LB, Levchenko, V, Ridd, PV, Rowe, C, Whinney, J, Wurster, CM and Zwart, C (2019) Identifying the 'savanna' signature in lacustrine sediments in northern Australia. *Quaternary Science Reviews* 203: 233-247, DOI:10.1016/j.quascirev2018.11.002.

Blaauw, M, Andres Christen, J, Esuivel Vazquez, J, Belding, T, Theiler, J, Gough, B and Karney, C (2019) Package 'rbacon'. Available at: https://cran.r-project.org/web/packages/rbacon/rbacon.pdf (accessed 1 July 2019).

Black, MP, Mooney, SD and Haberle, SG (2007) The fire, human and climate nexus in the Sydney Basin, eastern Australia', *The Holocene* 17(4): 469-480.

Bliege Bird, R, Bird, DW, Codding, BF, Parker, CH and Jones, JH (2008) The "fire stick farming" hypothesis: Australian Aboriginal foraging strategies, biodiversity, and anthropogenic fire mosaics. *Proceedings of the National Academy of Sciences of the United States of America* 105(39): 14796-14801.

Bliege Bird, R, Codding, BF, Kauhanen, PG and Bird, DW (2012) Aboriginal hunting buffers climate-driven fire-size variability in Australia's spinifex grasslands. *Proceedings of the National Academy of Sciences of the United States of America* 109(26): 10287-10292.

Bliege Bird, R, Tayor, N, Codding, BF and Bird, DW (2013) Niche construction and Dreaming logic: Aboriginal patch mosaic burning and varanid lizards (*Varanus gouldii*) in Australia. *Proceedings of the Royal Society B* 280: article no. 20132297.

Bliege Bird, R, Bird, DW and Codding, BF (2016) People, El Niño southern oscillation and fire in Australia: Fire regimes and climate controls in hummock grasslands. *Philosophical Transactions of the Royal Society B* 371: article no. 20150343.

Bowman, DMJS and Panton, WJ (1993) Decline of *Callitris intratropica* (RT Baker and HG Smith) in the Northern Territory: Implications for pre-and post-European colonization fire regimes. *Journal of Biogeography* 20: 373-381.

Bowman, DMJS, Walsh, A and Prior, LD (2004) Landscape analysis of Aboriginal fire management in Central Arnhem land, north Australia. *Journal of Biogeography* 31: 207-223.

Bureau of Meteorology (2020). Monthly Climate Statistics: Groote Eylandt Airport. Available at: http://www.bom.gov.au/climate/averages/tables/cw_014518.shtml (accessed 1 February 2020).

Clark, JS (1988) Particle motion and the theory of charcoal analysis: Source area, transport, deposition, and sampling. *Quaternary Research* 30: 67-80.

Clarkson, C, Jacobs, Z, Marwick, B, Fullagar, R, Wallis, L, Smith, M, Roberts, RG, Hayes, E, Lowe, K, Carah, X, Florin, SA, McNeil, J, Cox, D, Arnold, LJ, Hua, Q, Huntley, J, Brand, HEA, Manne, T, Fairbairn, A, Shulmeister, J, Lyle, L, Salinas, M, Page, M, Connell, K, Park, G, Norman, K, Murphy, T and Pardoe, C (2017) Human occupation of northern Australia by 65,000 years ago. *Nature* 547: 306-310.

Cole, K (1982) *A History of Numbulwar*. Victoria: Keith Cole Publications.

Courtney Mustaphi, CJ and Pisaric, MF (2014) A classification for macroscopic charcoal morphologies found in Holocene lacustrine sediments. *Progress in Physical Geography* 38(6): 734-754.

Crawford, AJ and Belcher, CM (2014) Charcoal morphometry for palaeoecological analysis: The effects of fuel type and transportation on morphological parameters. *Applications in Plant Sciences* 2(8): article no. 1400004.

Davies, SJ, Lamb, HF and Roberts, SJ (2015) Micro-XRF core scanning in palaeolimnology: Recent developments. In Croudace IW and Rothwell RG (eds) *Micro-XRF Studies of Sediment Cores: Applications of a non-destructive tool for the environmental sciences.* New York: Springer, pp. 189-226.

De Oliceria Goday, JM (1983) *Development of an analytical method for the determination of ^{238}U, ^{234}U, ^{232}Th, ^{230}Th, ^{228}Th, ^{228}Ra, ^{226}Ra, ^{210}Pb and ^{210}Po and its applications to environmental samples*. Karlsruhe: KFK 3502, Kernforschangszentrum.

Department of the Environment and Energy (2017) *NVIS Fact Sheet: MVG 3 – Eucalypt Open Forest*. Report, Australian Government, Canberra, Australia.

Diaz, HF and Markgraf, V (1992) *El Niño: Historical and Paleoclimatic Aspects of the Southern Oscillation*. Cambridge: Cambridge University Press.

Dowdy, AJ and Kuleshov, Y (2014) Climatology of lightning activity in Australia: Spatial and seasonal variability. *Australian Meteorological and Oceanographic Journal* 64: 103-108.

Duffin, KI, Gillson, L and Willis, KJ (2008) Testing the sensitivity of charcoal as an indicator of fire events in savanna environments: Quantitative predictions of fire proximity, area and intensity. *The Holocene* 18(2): 279-291.

Duyfken Replica Foundation (2016) Carstenzoon 1623. Available at: http://www.duyfken.com/Dutch%20mariners/carstenszoon-1623 (accessed 1 March 2018).

Eakins, JD and Morrison, RT (1978) A new procedure for the determination of lead-210 in lake and marine sediments. *International Journal of Applied Radiation and Isotopes* 29: 531-536.

Ekblom, A and Gillson, L (2010) Fire history and fire ecology of Northern Kruger (KNP) and Limpopo National Park (PNL), southern Africa. *The Holocene* 20(7): 1063-1077.

Enache, MD and Cumming BF (2006) Tracking recorded fires using charcoal morphology from the sedimentary sequence of Prosser Lake, British Columbia (Canada). *Quaternary Research* 65: 282-292.

Enright, NJ and Thomas, I (2008) Pre-European fire regimes in Australian ecosystems. *Geography Compass* 2(4): 979-1011.

Faulkner, P (2013) *Life on the Margins: An Archaeological Investigation of Late Holocene Economic Variability, Blue Mud Bay, Northern Australia.* Canberra: Terra Australis 38, ANU E Press.

Faulkner, P and Clarke, A (2004) Late-Holocene occupation and coastal economy in Blue Mud Bay, northeast Arnhem Land: Preliminary archaeological findings. *Australian Archaeology* 59: 23-30.

Field, E, McGowan, HA, Moss, PT and Marx, SK (2017) A late Quaternary record of monsoon variability in the northwest Kimberley, Australia. *Quaternary International* 449: 119-135.

Fink, D, Hotchkis, M, Hua, Q, Jacobsen, G, Smith, AM, Zoppi, U, Child, D, Mifsud, C, van der Gaast, H, Williams, A and Williams, M (2004) The ANTARES AMS facility at ANSTO. *Nuclear Instruments and Methods in Physics Research Section B: Beam Interactions with Materials and Atoms* 223-224: 109-115.

Flinders, M (1966) Voyage to Terra Australis. Available at: https://gutenberg.net.au/ebooks/e00049.html (accessed 12 August 2016).

Fox, ID, Neldner, VJ, Wilson, GW and Bannink, PJ (2001) *The Vegetation of the Australian Tropical Savannas*. Brisbane: Queensland Government.

Gambold, NJ (2015) *South East Arnhem Land Indigenous Protected Area: Plan of Management 2016-2021*. Report, Northern Land Council, Darwin, Northern Territory, Australia.

Gammage, B (2012) *The Biggest Estate on Earth.* Sydney: Allen and Unwin.

Golding, AS (1961) Determination of dissolved radium. *Analytical Chemistry* 33: 406.

Google Earth (2020) Marura sinkhole, Arnhem Land, Northern Territory, 13°24'34"S, 135°46'29"E, elevation 50m. Available at: https://earth.google.com/web/@-13.41568201,135.78226053,44.58781274a,32267.31239995d,35y,-0h,0t,0r (accessed 17 February 2020).

Haberle, SG (2005) A 23,000-yr pollen record from Lake Euramoo, Wet Tropics of NE Queensland, Australia. *Quaternary Research* 64: 343-356.

Haines, PW, Rawlings, D, Sweet, I, Pietsch, B, Plumb, K, Madigan, T and Krassay, A (1999) *Blue Mud Bay, Northern Territory: 1:250 000 scale geological series, explanatory notes*. Darwin: Northern Territory Geological Survey.

Head, L (1994) Landscapes socialised by fire: Post-contact changes in Aboriginal fire use in northern Australia, and implications for prehistory. *Archaeology in Oceania* 29(3): 172-181.

Head, L and Fullager, R (1992) Palaeoecology and archaeology in the east Kimberley. *Quaternary Australasia* 10(1): 27-31.

Heeres, JE (1899) The Part Borne by the Dutch in the Discovery of Australia 1606-1765. Available at: https://www.gutenberg.org/files/17450/17450-h/17450-h.htm (accessed 20 September 2018).

Higuera, PE, Sprugel, DG and Brubaker, LB (2005) Reconstructing fire regimes with charcoal from small-hollow sediments: A calibration with tree-ring records of fire. *The Holocene* 15(2): 238-251.

Hiscock, P and Kershaw, AP (1992) Palaeoenvironments and prehistory of Australia's tropical Top End. In Dodson J (ed) *The Naive Lands: Prehistory and Environmental Change in Australia and the South-west Pacific*. Melbourne: Longman Cheshire, pp. 43-75.

Hogg, AG, Hua, Q, Blackwell, PG, Niu, M, Buck, CE, Guilderson, TP, Heaton, TJ, Palmer, JG, Reimer, PJ, Reimer, RW, Turney, CSM, Zimmerman, SRH (2013) SHCAL13 Southern Hemisphere calibration, 0-50,000 years cal BP. *Radiocarbon* 55(4): 1889-1903.

Hua, Q, Jacobsen, GE, Zoppi, U, Lawson, EM, Williams, AA, Smith, AM and McGann, MJ (2001) Progress in radiocarbon target preparation at the ANTARES AMS Centre. *Proceedings of the 17th International Radiocarbon Conference* 43(2A): 275-282.

International Commission on Stratigraphy (2019) ICS v2019/05. Available at: http://stratigraphy.org/ICSchart/ChronostratChart2019-05.pdf (accessed 7 October 2019).

Iversen, J (1941) Landnam i Danmarks stenalder (Land occupation in Denmark's Stone Age). *Danmarks Geologiske Undersogelse* 66: 1-68.

Johnson, CN (2016) Fire, people and ecosystem change in Pleistocene Australia. *Australian Journal of Botany* 64(8): 643-651.

1 Keeley, JE (2009) Fire intensity, fire severity and burn severity: A brief review and suggested
2 usage. *International Journal of Wildland Fire* 18: 116-126.

3 Kershaw, AP, Clark, JS, Gill, AM and D'Costa, AM (2002) A history of fire in Australia. In
4 Bradstock RA, Williams JE and Gill AM (eds) *Flammable Australia: The Fire Regimes and*
5 *Biodiversity of a Continent*. Cambridge: Cambridge University Press, pp. 3-25.

6 Lewis, SE, Sloss, CR., Murray-Wallace, CV., Woodroffe, CD., and Smithers, SG (2013) Post-
7 glacial sea-level changes around the Australian margin: a review. *Quaternary Science Reviews*
8 74: 115-138.

9 Leys, B, Brewer, SC, McConaghy, S, Mueller, J and McLauchlan, KK (2015) Fire history
10 reconstruction in grassland ecosystems: Amount of charcoal reflects local area burned.
11 *Environmental Research Letters* 10: article no. 114009.

12 Leys, BA, Commerford, JL and McLauchlan, KK (2017) Reconstructing grassland fire history
13 using sedimentary charcoal: Considering count, size and shape. *PLoS ONE* 12(4): article no.
14 e0176445.

15 Lim, TP and Dave, NK (1981) A rapid method of ^{226}Ra analysis in water samples using an
16 alpha-spectrometric technique. *CIM Bulletin* 74: 97.

17 Lim, TP, Dave, NK and Cloutier, NR (1989) High resolution alpha spectrometry for radium
18 analysis – The effects of sample thickness and filter pore size. *International Journal of Applied*
19 *Radiation and Isotopes* 40(1A): 63-71.

20 Masiello, CA (2004) New directions in black carbon organic geochemistry. *Marine Chemistry*
21 92: 201-213.

McGowan, H, Marx, S, Moss, P and Hammond, A (2012) Evidence of ENSO mega-drought triggered collapse of prehistory Aboriginal society in northwest Australia. *Geophysical Research Letters* 39: article no. L22702.

McMillan, A (2008) *An Intruder's Guide to East Arnhem Land.* Nightcliff, Northern Territory: Niblock Publishing.

Meredith, W, Ascough, PL, Bird, MI, Large, DJ, Snape, CE, Sun, Y and Tilston, EL (2012) Assessment of hydropyrolysis as a method for the quantification of black carbon using standard reference materials. *Geochimica et Cosmochimica Acta* 97: 131-147.

Mooney, SD and Tinner, W (2011) The analysis of charcoal in peat and organic sediments. *Mires and Peat* 7: 1-18.

Mooney, SD, Harrison, SP, Bartlein, PJ, Daniau, A-L, Stevenson, J, Brownlie, KC, Buckman, S, Cupper, M, Luly, J, Black, M, Colhoun, E, D'Costa, D, Dodson, J, Haberle, S, Hope, GS, Kershaw, P, Kenyon, C, McKenzie, M and Williams, N (2011) Late Quaternary fire regimes of Australasia. *Quaternary Science Reviews* 30: 28-46.

Moss, P, Mackenzie, L, Ulm, S, Sloss, C, Rosendahl, D, Petherick, L, Steinberger, L, Wallis, L, Heijnis, H, Petchey, F and Jacobsen, G (2015) Environmental context for late Holocene human occupation of the South Wellesley Archipelago, Gulf of Carpentaria, northern Australia. *Quaternary International* 385: 136-144.

National Archives of Australia (2018) Commonwealth Government Records about the Northern Territory Part 1: 1.4 Establishment of the Pastoral Industry. Available at: http://guides.naa.gov.au/records-about-northern-territory/part1/chapter1/1.4.aspx (accessed 20 September 2018).

National Museum of Australia (2018) Old Masters: Arnhem Land. Available at: http://www.nma.gov.au/exhibitions/old_masters/arnhem_land (accessed 1 June 2018).

Northcote, KH, Beckmann, GG, Bettenay, E, Churchward, HM, Van Dijk, DC, Dimmock, GM, Hubble, GD, Isbell, RF, McArthur, WM, Murtha, GG, Nicolls, KD, Paton, TR, Thompson, CH, Webb, AA and Wright, MJ (1960-1968) *Atlas of Australian Soils, Sheets 1 to 10 with Explanatory Data*. Melbourne: Commonwealth Scientific and Industrial Research Organisation and Melbourne University Press.

Northern Australian Fire Information [NAFI] (2020) Fire History – North Australia and Rangelands Fire Information. Available at: https://www.firenorth.org.au/nafi3/ (accessed 1 February 2020).

Nott, J and Price, D (1994) Plunge pools and paleoprecipitation. *Geology* 22: 1047-1050.

O'Leary, MH (1988) Carbon isotopes in photosynthesis. *BioScience* 38(5): 328-336.

Perry, GLW, Wilmshurst, JM and McGlone, MS (2014) Ecology and long-term history of fire in New Zealand. *New Zealand Journal of Ecology* 38(2): 157-176.

Peters, ME and Higuera, PE (2007) Quantifying the source area of macroscopic charcoal with a particle dispersal model. *Quaternary Research* 67: 304-310.

Plumb, KA and Roberts, HG (1967) *Explanatory Notes on the Blue Mud Bay – Port Langdon 1:250,000 Geological Series Sheet SD53-7/8: Records 1964/67*. Canberra: Bureau of Mineral Resources, Geology and Geophysics and Commonwealth Government of Australia.

Prebble, M, Sim, R, Finn, J and Fink, D (2005) A Holocene pollen and diatom record from Vanderlin Island, Gulf of Carpentaria, lowland tropical Australia. *Quaternary Research* 64: 357-371.

1 Preece, N (2002) Aboriginal fires in monsoonal Australia from historical accounts. *Journal of*
2 *Biogeography* 29: 321-336.

3 Proske, U and Haberle, SG (2012) Island ecosystem and biodiversity dynamics in northeastern
4 Australia during the Holocene: Unravelling short-term impacts and long-term drivers. *The*
5 *Holocene* 22(10): 1-15.

6 Pyne, SJ (1991) *Burning Bush.* New York: Henry Holt and Company.

7 R Development Core Team (2013) *R: A language and environment for statistical computing.*
8 Vienna: R Foundation for Statistical Computing.

9 Rowe, C (2007) A palynological investigation of Holocene vegetation change in Torres Strait,
10 seasonal tropics of northern Australia. *Palaeogeography, Palaeoclimatology, Palaeoecology*
11 251: 83-103.

12 Rowe, C, Brand, M, Hutley, LB, Wurster, C, Zwart, C, Levchenko, V and Bird, M (2019)
13 Holocene savanna dynamics in the seasonal tropics of northern Australia. *Review of*
14 *Palaeobotany and Palynology* 267: 17-31.

15 Russell-Smith, J and Yates, CP (2007) Australian savanna fire regimes: Context, scales,
16 patchiness. *Fire Ecology Special Issue* 3(1): 48-63.

17 Russell-Smith, J, Lucas, D, Gapindi, M, Gunbunuka, B, Kapirigi, N, Namingum, G, Lucas, K,
18 Giuliani, P and Chaloupka, G (1997) Aboriginal resource utilization and fire management
19 practice in western Arnhem Land, monsoonal northern Australia. *Human Ecology* 25(2): 159-
20 195.

21 Russell-Smith, J, Yates, C, Edwards, A, Allan, GE, Cook, GD, Cooke, P, Craig, R, Heath, B
22 and Smith, R (2003) Contemporary fire regimes of northern Australia, 1997–2001: Change

since Aboriginal occupancy, challenges for sustainable management. *International Journal of Wildland Fire* 12: 283-297.

Saiz, G, Goodrick, I, Wurster, C, Nelson, PN, Wynn, J and Bird, M (2018) Preferential production and transport of grass-derived pyrogenic carbon in NE-Australian savanna ecosystems. *Frontiers in Earth Science* 5: 1-13.

Shulmeister, J (1992) A Holocene pollen record from lowland tropical Australia. *The Holocene* 2(2): 107-116.

Shulmeister, J (1999) Australasian evidence for mid-Holocene climate change implies precessional control of Walker Circulation in the Pacific. *Quaternary International* 57/58: 81-91.

Shulmeister, J and Lees, BG (1995) Pollen evidence from tropical Australia for the onset of an ENSO-dominated climate at c. 4000 BP. *The Holocene* 5(1): 10-18.

Sloss, CR, Nothdurft, L, Hua, Q, O'Connor, SG, Moss, PT, Rosendahl, D, Petherick, LM, Nanson, RA, Mackenzie, LL, Sternes, A, Jacobsen, GE, and Ulm, S (2018) Holocene sea-level change and coastal landscape evolution in the southern Gulf of Carpentaria, Australia. *The Holocene* 28(9): 1411-1430.

Stevenson, J and Haberle, S (2005) *Macro charcoal analysis: A modified technique used by the Department of Archaeology and Natural History.* Palaeoworks Technical Papers 5. Canberra: Australian National University.

Stevenson, J, Brockwell, S, Rowe, C, Proske, U and Shiner, J (2015) The palaeoenvironmental history of Big Willum Swamp, Weipa: An environmental context for the archaeological record. *Australian Archaeology* 80: 17-31.

Sydney Morning Herald (2004) Arnhem Land. Available at: https://www.smh.com.au/lifestyle/arnhem-land-20040208-gdkqam.html (accessed 20 September 2018).

Taçon, PSC, May, SK, Fallon, SJ, Travers, M, Wesley, D, and Lamilami, R (2010) A minimum age for early depictions of Southeast Asian praus in the rock art of Arnhem Land, Northern Territory. *Australian Archaeology* 71: 1-10.

Thevenon, F, Williamson, D, Bard, E, Anselmetti, FS, Beaufort, L and Cachier, H (2010) Combining charcoal and elemental black carbon analysis in sedimentary archives: Implications for past fire regimes, the pyrogenic carbon cycle, and the human-climate interactions. *Global and Planetary Change* 72: 381-389.

Trauernicht, C, Brook, BW, Murphy, BP, Williamson, GJ and Bowman, DMJS (2015) Local and global pyrogeographic evidence that indigenous fire management creates pyrodiversity. *Ecology and Evolution* 5(9): 1908-1918.

Umbanhowar, CE and McGrath, MJ (1998) Experimental production and analysis of microscopic charcoal from wood, leaves and grasses. *The Holocene* 8(3): 341-346.

Weltje, GJ, Bloemsma, MR, Tjallingii, R, Heslop, D, Röhl, U and Croudace, IW (2015) Prediction of geochemical composition from XRF core scanner data: A new multivariate approach including automatic selection of calibration samples and quantification uncertainties. In Croudace IW and Rothwell RG (eds) *Micro-XRF Studies of Sediment Cores: Applications of a non-destructive tool for the environmental sciences*. Developments in Paleoenvironmental Research 17. New York: Springer.

Williams, AN (2013) A new population curve for prehistoric Australia. *Proceedings of the Royal Society B* 280: article no. 20130486.

Williams, AN, Mooney, SD, Sisson, SA and Marlon, J (2015) Exploring the relationship between Aboriginal population indices and fire in Australia over the last 20,000 years. *Palaeogeography, Palaeoclimatology, Palaeoecology* 432: 49-57.

Williams, RJ, Gill, AM and Moore, PHR (1998) Seasonal changes in fire behaviour in a tropical savanna in northern Australia. *International Journal of Wildland Fire* 8(4): 227-239.

Woodward, CA and Gadd, PS (2019) The potential power and pitfalls of using the X-ray fluorescence molybdenum incoherent: Coherent scattering ratio as a proxy for sediment organic content. *Quaternary International* 514: 30-43.

Wurster, CM, Lloyd, J, Goodrick, I, Saiz, G and Bird, MI (2012) Quantifying the abundance and stable isotope composition of pyrogenic carbon using hydrogen pyrolysis. *Rapid Communications in Mass Spectrometry* 26: 2690-2696.

Wurster, CM, Saiz, G, Schneider, MPW, Schmidt, MWI and Bird, MI (2013) Quantifying pyrogenic carbon from thermosequences of wood and grass using hydrogen pyrolysis. *Organic Geochemistry* 62: 28-32.

Wyrwoll, K-H and Miller, GH (2001) Initiation of the Australian summer monsoon 14,000 years ago. *Quaternary International* 83-85: 119-128.

Yibarbuk, D, Whitehead, PJ, Russell-Smith, J, Jackson, D, Godjuwa, C, Fisher, A, Cooke, P, Choquenot, D and DMJS Bowman (2001) Fire ecology and Aboriginal land management in central Arnhem Land, northern Australia: A tradition of ecosystem management. *Journal of Biogeography* 28: 325-343.